Time-resolved measurement technique for pulsed electron beam envelope basing on framing and streaking principle*

Xiao-Guo Jiang(江孝国)[1)] Yuan Wang(王远) Zhi-Yong Yang(杨治勇) Huang Zhang(张篁) Yi Wang(王毅)

Institute of Fluid Physics，China Academy of Engineering Physics, Mianyang 621900, China

Abstract: The time-resolved electron beam envelope parameters, including cross sectional distribution and beam centroid position, are very important for the study of beam transmission characteristics in a magnetic field and for verifying the rationality of the magnetic field parameters employed. One kind of high time-resolved beam envelope measurement system has recently been developed, constituted of a high-speed framing camera and a streak camera. It can obtain three panoramic images of the beam and time continuous information along the given beam profile simultaneously. Recently obtained data has proved that several fast vibrations of the beam envelope along the diameter direction occur during the front and the tail parts of the electron beam. The vibration period is several nanoseconds. The effect of magnetic field on the electron beam is also observed and verified. Beam debugging experiments have proved that the existing beam transmission design is reasonable and viable. This beam envelope measurement system will establish a good foundation for beam physics research.

Keywords: high-speed framing camera, streak camera, beam envelope, time-resolved measurement

PACS: 41.85.Ja, 41.85.Ew, 29.27.Eg **DOI:** 10.1088/1674-1137/40/1/017003

1 Introduction

The linear induction accelerator (LIA) is one kind of accelerator which is often used to accelerate high-current electron beams of up to several kiloamperes. The intense pulsed electron beam must be well restricted by a strong magnetic field within the central area of the accelerating cavity, which is several centimeters in diameter. Also, the electron beam should be transmitted with as little loss as possible from the injector to the exit of the accelerator. This distance is about several tens of meters. This demand for high efficiency is a big challenge for long-distance beam transport techniques. The most important work for beam transport in the injector is achieving the best configuration of matched magnetic field. A mismatched magnetic field configuration at the injector stage or the first accelerating cavity will have a serious influence on transmission of the beam in the following stages. The focusing force or the ability to restrict the electron beam will obviously vary with the electron energy and the emission status of the electron from the thermionic cathode at the injector [1, 2]. This results in electrons with different energies moving along different tracks inside the cavity, and in the beam envelope varying markedly under certain mismatched magnetic field configurations. Initial simulations show that the electron beam envelope shrinks and enlarges turbulently during the front and tail ends of the electron beam pulse. There are usually about 3–5 vibration periods during about 20 nanoseconds. Because of the turbulent beam envelope vibration, some electrons may hit the cavity wall and be lost. An electron beam with better characteristics may be obtained if we allow the unwanted electron current to be lost voluntarily at some certain position by adjusting the magnetic field configuration. The lost electron current is likely to bring some ill effect to the following beam transmission, however. On the other hand, the electron beam envelope may be well restricted under some matched magnetic field configuration and can be transported to the next segment without electron loss or electron beam envelope vibration. Time-resolved measurement technology, especially for the electron beam envelope, is the key technology to debug such an electron beam. It is very difficult to obtain about 5 periods of vibrations during the 20 nanoseconds at both ends of the beam pulse, however. The time-resolved measurement ability and the image frames obtained are critical limiting factors for the measurement system to obtain detailed information about the changes in the electron beam envelope. Based on our previously developed time-resolved measurement system [3–7] and the existing design principle, a composite measurement system

Received 6 February 2015, Revised 22 July 2015

∗ Supported by National Natural Science Foundation of China (10675104, 11375162)

1) E-mail: J_xg_caep@sina.com

for electron beam envelopes is developed by combining a high speed framing camera and a streak camera. Several panoramic images of the electron beam envelope at different times and the profile image of the center slit of the electron beam over the whole pulse duration can be obtained at the same time. The framing images are captured by the high speed framing camera with several nanoseconds shutter time. The interval time between the framing images can reach 3 – 5 ns. The profile image is captured by the streak camera. The time-resolved ability for the profile image can reach sub-nanosecond level, restricted by the streak camera. This measurement ability can meet the demands of obtaining the turbulent changes of the beam envelope at both ends of the beam pulse as mentioned above.

This measurement technology has been successfully applied in beam debugging and beam transmission at the injector. It has provided plentiful experiment data including intuitive and exact images for the debugging work of the magnetic field configuration at the injector. It has established a good foundation for obtaining the beam vibration. It also provides the ability to measure experimentally and validate the debug work to achieve the best matched magnetic field configuration, as well as to study the beam transmission theory.

2 Structure of the time-resolved measurement system

Figure 1 shows the structure of the time-resolved beam envelope measurement system. It consists of an optical transition radiation (OTR) target [8], a light beam splitting component, a high speed framing camera and a high speed streak camera.

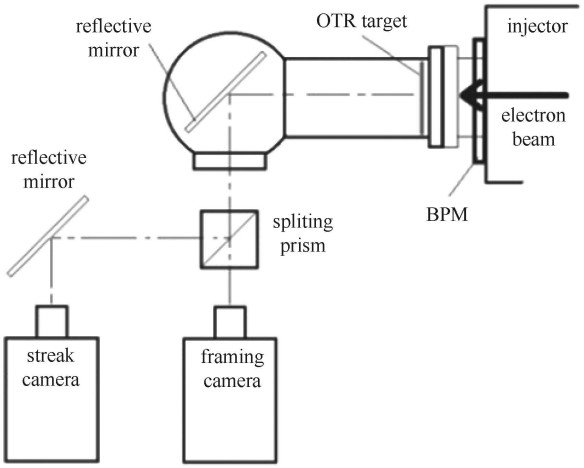

Fig. 1. Layout of time-resolved electron beam measurement.

The highest time-resolved ability of this system is mainly determined by the speed of the cameras. The framing camera is able to capture 3 frame images at one time, with a minimum shutter time up to about 2 ns. The streak camera usually works at a sweep speed of about 0.2 ns/point, which can reach a high temporal system resolution of up to about 2 ps at the highest speed. The time-resolved ability of the whole system can meet the framing and streak imaging demands with a speed high enough for a pulsed electron beam with a duration of about 100 ns. The BPM marked in Fig. 1 is a beam position monitor, which is used to measure the beam current and the beam centroid position. The BPM is located 500 mm upstream from the OTR target.

3 Electron beam envelope study with time-resolved measurement

The electron beam emitting from the thermionic cathode usually covers a wide energy spectrum and has some transverse angular momentum. All these factors will gradually undermine the beam transport or acceleration and must be solved at the injector stage. In the injector, the electron beam runs into the anode cavity after being emitted from the thermionic cathode, then begins its transportation. In this segment, it is hoped to transport the electron beam with as little loss as possible. It is also hoped that the beam envelope will change as little as possible and the beam can be stably transported to the acceleration segment. This can help to restrain beam emittance growth, which is important for the following transmission and acceleration. How to configure the magnetic field at the injector segment becomes an important research topic. The degree of matching of the magnetic field will obviously affect the electron beam transmission efficiency. Theoretical simulation work was therefore carried out using the actual structure of the diode in the injector, aiming at the temporal continuity of the beam envelope. The beam envelope was also measured under the corresponding conditions, obtaining a series of results. This simulation work plays an important role in analyzing the effect of the magnetic field and validating the simulation program.

Typical simulation results of the beam envelope profile continuous change with time are shown in Fig. 2. In order to be temporally associated with the beam current waveform, the current amplitude is normalized and the position is offset. The simulation is aimed at the beam envelope change at a downstream position 4900 mm from the cathode surface over about 150 ns. The simulation starts at 0 ns. The simulation results show that there are several vibrations during the front and the tail end of the electron beam pulse. These phenomena were not observed in previous experiments. The simulation results show that the beam envelope will change obviously under different magnetic field configurations. The beam

diameter can be large or small during the front and the tail end of the pulse. The beam envelope can also change in different patterns. All these may severely affect the following transport. It is very important to find the ways in which the beam envelope changes.

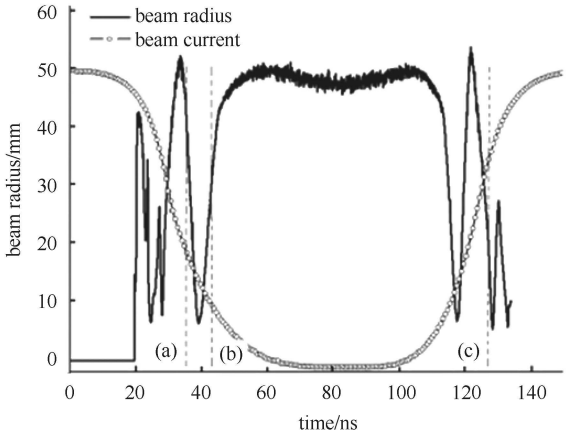

Fig. 2. Change of simulated beam envelope with time.

Figure 3 shows some typical framing and streak images of the electron beam at the exit of the injector. The image contrast and image gray are adjusted to give an optimized visual impression. Images (a), (b) and (c) are framing images. Images (a) and (b) are captured during the forepart of the beam pulse. The shutter opening monitor shows that the capture time of image (a) is at 36 ns and the capture time of image (b) is at 43 ns. Image (c) is captured during the tail end of the beam pulse. The capture time of image (c) is at 127 ns. All shutter times for the above framing images are 5 ns. The image capture time associated with the beam current waveform is shown in Fig. 2.

The beam envelope images can be captured during the front and the tail end of the short duration of the electron beam pulse. However, there exist some difficulties which prevent us from obtaining the entire course of the beam envelope vibration or very detailed information about the vibration, including: (1) Only three frames can be captured by the framing camera in total, which is far from enough if we want to observe the whole course of the pulse; (2) An integral image within certain pulse duration is actually obtained if a wider shutter time is adopted to capture the rapid vibration image. This is one main factor for the beam image appearing to be layered sometimes; (3) With a shorter shutter time, because of its low contrast and poor differentiation ability, the image is usually too weak to provide enough information; (4) It is very difficult to synchronize the shutter with the beam pulse edge at ns level because the trigger synchronization precision of the framing camera is about 5 ns under the LIA environment. The streak camera has the advantages of a continuous rapid sweep and low synchronization accuracy demand for trigger. Image (d) in Fig. 3 is the streak image of the electron beam profile over the whole beam pulse. The slit was adjusted so that the streak camera would image the beam profile at the middle position. The image captured provides diameter information about the beam profile along the beam axis. The streak image shows that there are several beam vibrations during the front and tail ends of the beam pulse. The beam diameter during the pulse middle also changes.

At the injector, whether the electrons run into the cavity wall or not will significantly affect the following acceleration and transmission. Some validation experiments were designed to study this phenomenon. In the experiments, the BPM in the inner injector cavity was utilized as a beam mask aperture. The unique shape of the BPM helps it to detect the edge of the beam profile. With a given spatial distribution, the 48 resistances forming the BPM are ranged in parallel along the radial direction. A correlation of beam profile with the BPM ring structure may be produced if the electrons run into the cavity wall at the BPM position.

A set of magnetic field configurations which will cause electrons to hit the wall at the BPM was obtained by the PIC simulation program and the corresponding experiments were carried out. Figure 4 shows the typical beam envelope images captured in the experiments. Fig. 4(a) and (b) are two images of the front part of the pulse captured by framing camera. Image (a) was captured

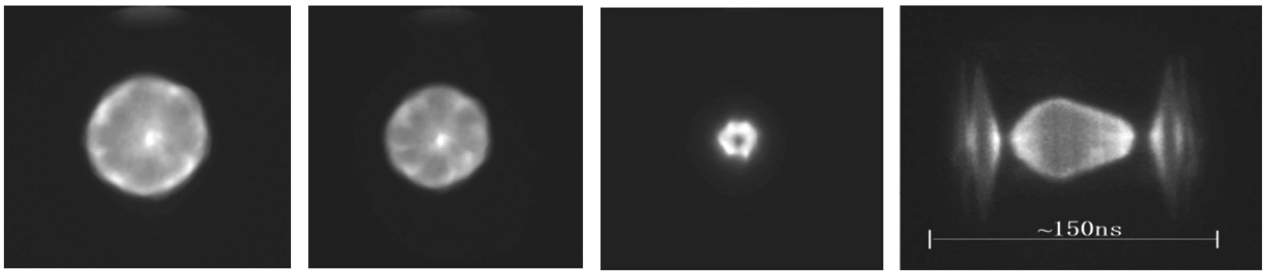

Fig. 3. Typical time-resolved framing images and streak camera image of electron beam from the injector.

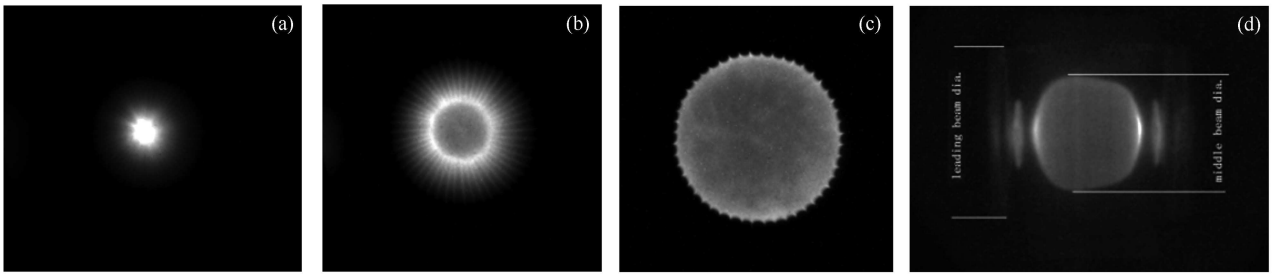

Fig. 4. Typical images produced when the electron beam collides with the inner wall at the BPM.

about 8 ns earlier than image (b), and both of them were taken between the 20 ns and 30 ns section of Fig. 2. Figure 4(b) is within the last vibration before the flat top of the beam pulse. Figure 4(c) shows the beam envelope during the flat top. All shutter times for these images are 5 ns. These experiment phenomena can be reliably reproduced.

The beam current loss, which is measured by the BPM at the exit of the injector, is obvious compared with the emission current at the surface of the thermionic cathode. The beam current waveform shows that the current loss during the front and tail ends is especially large and that during the flat top is relatively small. This indicates that many electrons collide with the wall. The 48-toothed fringe and 48 spokes in Fig. 4(a), (b) and (c) indicate that the collision location may be at the BPM. The OTR target should be fixed close to the BPM to avoid beam shape distortion. The beam profile on the whole keeps its previous shape, without obvious divergence or convergence, after it passes the BPM. While the three images show evolution of the electron beam profile, the mechanism for the rapid vibration is not yet clear.

Under this magnetic field configuration, the streak image shows that the diameter of the electron beam at the front part of the pulse goes beyond that of the inner wall of the cavity. Collision becomes inevitable. The beam diameter during the flat top section decreases gradually and slowly, shown as Fig. 4(d).

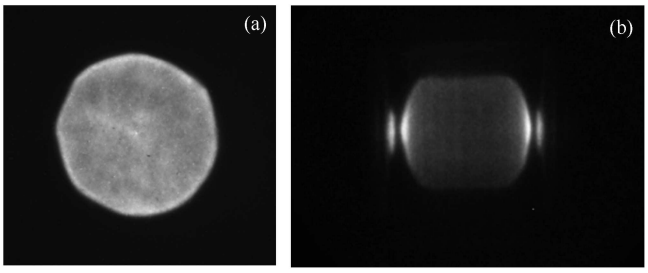

Fig. 5. Verification images of electron beam transmission without loss through the injector.

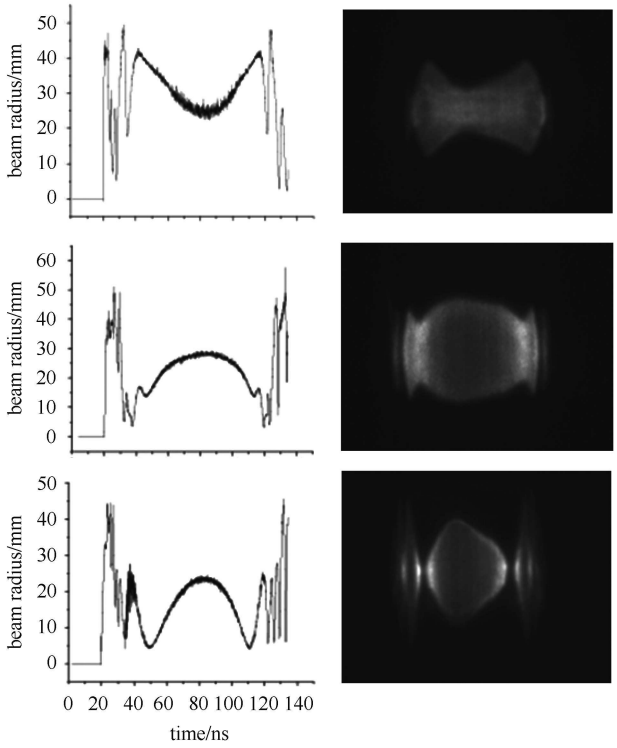

Fig. 6. Several simulated beam envelopes and the corresponding practical streak images under different magnetic fields.

The above simulation work provides a feasible way to control the beam envelope effectively. Other parameters of the magnetic field configuration are also simulated in order to transport the electron beam without loss. The objective is to ensure that the electrons are restricted in the central area of the accelerating cavity without loss. This demands that the electron beam profile diameter should be smaller than that of the cavity. In this case, the beam envelope changes slowly without any turbulence. In the experiments, the typical images captured are shown in Fig. 5. Figure 5(a) is a framing image captured at the flat top section of the beam pulse with 5 ns shutter time. Figure 5(b) is a streak image captured by the streak camera with 200 ns sweep time. We can see that the beam envelope vibrations in Fig. 5(b) have amplitude and intensity much smaller than those in

Fig. 4(d) during the front and tail ends, while the beam diameter during the flat top section of the pulse is stable and the beam profile has good uniformity. These results have proved that the magnetic field configuration meets the requirements. Later beam transport and focusing work testified again to this improved effect.

More experiments with different sets of magnetic field configuration were taken at the injector. The results are consistent with theoretical simulations, as shown in Fig. 6; the curves are simulation results of beam envelope vibration and the pictures are corresponding streak images. In general, the simulation results match the actual images better in the main section of the pulse.

4 Discussion

The images, especially those captured with the streak camera, show that there exist envelope vibrations during the front and tail ends of the pulse which can be turbulent under certain conditions. Even within the same pulse, the vibration amplitude and duration can vary. Theoretically, experimental requirements can be achieved to an acceptable extent by adjusting the magnetic field configuration. The experiment results show good consistency with the simulation. Thus we have the ability in simulations of intense pulsed electron beam transmission in the injector. This is very helpful in debugging work for pulsed electron beams of several kiloamperes current. This may be the most fruitful result from this paper.

There are still some problems, however. Observing carefully, we find there is some difference between the actual images and the simulation results. The number of vibrations observed may be different from the simulation results, and the shapes of the beam envelope have some differences. There are two main reasons for these differences. First of all, it is difficult to exactly control the beam parameters at the cathode, so the input electron beam parameters for the theoretical simulation are, inevitably, not identical to those in the experiments, and sometimes the difference can be significant. Generally, these parameters include beam emittance, beam incidence angle, beam energy, beam current, current waveform, etc. The influence of beam emittance and beam incidence angle may be particularly important. Thus, a reasonable choice of these parameters becomes a key part of theoretical simulations. As a matter of fact, we never know the exact values of the parameters since it is difficult to measure them through experiments. The usual way to deal with this problem is to choose the input parameters by experience. The inconsistency between input parameters and real parameters lead to the mismatch between the simulation and the measurement. The other reason for the differences is that the image gray density in the extreme front and back of the pulse is too low to be detected. This results in the beam envelope being only faintly outlined. It is also difficult to clearly distinguish the number of vibrations. Under the same magnetic field, the difference in electron energy may induce differences in vibrating period and beam envelope diameter. Beam envelopes with different diameters and vibrating periods overlap with each other to blur the outline of the beam profile image. This kind of overlapping immediately results in electron density reduction or lower image gray-scale density. The width of the slit at the input window of the streak camera may be increased to produce enough image gray-scale. This is incompatible with the demands of high time-resolution ability or spatial resolution along the time axis in the image, which plays a decisive role in distinguishing the rapid beam envelope vibration. However, there are some measures that can be adopted to record the beam envelope vibration during the front and tail ends under specific conditions. For example, we can increase the sweep speed and only capture an image of one part of the duration. The results are shown in Fig. 7(b). Detailed information of the beam envelope at the given duration can be obtained and some information, such as the electron halo at the outer beam, is much clearer.

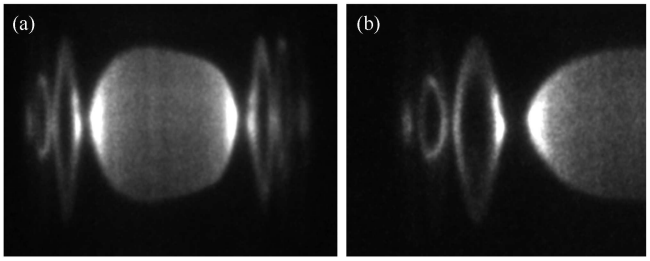

Fig. 7. Streak images focusing on the leading edge.

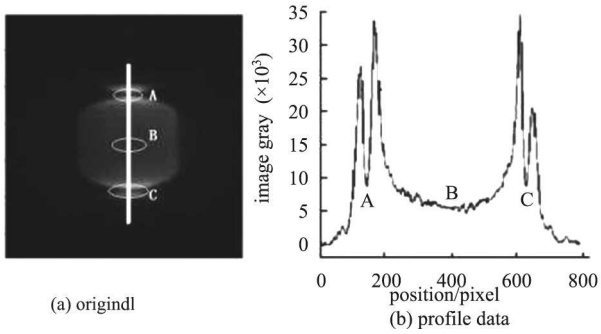

Fig. 8. Analysis of time continuity for the beam envelope.

Another confusing phenomenon in the streak image is in the part between the last vibration and the flat top, shown as point A and point C in Fig. 8(a). It seems as if there exists a discontinuity of electron beam at these parts in the image. In fact, the image gray level at these positions is at an upper level if we get the image gray

data, which may be even greater than that at the flat top section such as point B in the image, shown as Fig. 8(b). The image discontinuity in vision is merely a result of the remarkable differential contrast. Thus the electron beam is temporally continuous.

5 Conclusion

We have recently developed an electron beam envelope measurement system made up of a high-speed framing camera and a streak camera. When an OTR target is used, it can capture three time-resolved framing images and a streak image of the beam profile and envelope simultaneously. These images are complementary and can explain some phenomena more comprehensively. The successful development of this electron beam envelope measurement system provides a strong and useful means to study the pulsed intense electron beam and its transmission rule. The data recently obtained from experiments prove that several fast vibrations of the beam envelope along the diameter direction do occur during the front and tail ends of the electron beam. The vibration period is several nanoseconds. The effect of the magnetic field configuration on the electron beam transmission is also validated to some extent. The measurement work also proves that the existing beam transmission design is reasonable and viable. The theoretical simulation has immediate practical application in guiding electron beam debugging work. The far-reaching significance is that this system provides us with the ability to validate theoretical simulation results and is therefore a powerful method for beam physics research.

References

1 A. M. Yang, L. S. Xia, H. Zhang et al, Chin Phys C, **32**(S1): 286–288 (2008)
2 L. S. Xia, H. Zhang, X. G. Jiang et al, High Energy Physics and Nuclear Physics, **30**(5): 470–475 (2006) (in Chinese)
3 X. G. Jiang, X. N. Dong, Y. Wang et al, High Power Laser and Particle Beams, **22**(9): 2147–2150 (2010) (in Chinese)
4 X. G. Jiang, Y. Wang, K. Z. Zhang et al, High Power Laser and Particle Beams, **24**(5): 1146–1150 (2012) (in Chinese)
5 X. G. Jiang, Y. Wang, G. Jin et al, ACTA Photonica Sinica, **42**(9): 1065–1070 (2013)
6 X. G. Jiang, B. P. Guo, J. J. Deng et al, Opto-Electronic Engineering, **33**(5): 99–103 (2006)
7 X. G. Jiang, C. G. Li, Y. Wang et al, High Energy Physics and Nuclear Physics, **30**(8): 784–787 (2006) (in Chinese)
8 G. J. Yang, C. J. Liu, Y. Z. Lin et al, High Power Laser and Particle Beams, **16**(9): 1215–1218 (2004) (in Chinese)